Photon-assisted transmission through an oscillating quantum well: A transfer-matrix approach to coherent destruction of tunneling

Mathias Wagner
Hitachi Cambridge Laboratory, Madingley Road, Cambridge CB3 0HE, United Kingdom
(Received 13 June 1994)

Based on a transfer-matrix formalism, photon-assisted tunneling is studied in a strongly driven double-barrier tunneling diode. Two scenarios are considered: a driving potential $V_1\cos(\omega t)$ acting on the central quantum well, which may be realized with electrostatic gates close to the quantum well, and a driving electric field across the diode generated by a laser field. Strong quenching of the transmission probability is found for certain parameters $\{V_1,\omega\}$ of the driving field, which can be explained in terms of zeros of fractional Bessel functions, $J_{\pm\nu}(\gamma V_1/\hbar\omega)$, where γ is a structural parameter. The effect shows a strong similarity to the "coherent destruction of tunneling" recently found in strongly driven quartic double wells.

PACS number(s): 42.50.Ne, 03.65.Ge, 42.50.Hz, 73.20.Dx

I. INTRODUCTION

Harmonically driven bistable systems have recently attracted a great deal of interest in the field of nonlinear dynamics. In the classical regime, they exhibit instabilities and fractal phase-space structures with at least two, possibly strange, attractors [1], while in the quantum-mechanical regime they feature a rich variety of effects related to coherent tunneling. The archetype of strongly driven bistable systems is the harmonically driven symmetric quartic double well with $V(z)=-z^2/4+z^4/64D$, where the two lowest lying states are almost degenerate. Such a bistable system can, for instance, be realized in a laser-irradiated semiconductor double quantum well. In their pioneering work, Großmann *et al.* [2] showed that the coherent tunneling between the two lowest states of a quartic double well can be suppressed by many orders of magnitude, if the laser power and frequency are chosen carefully. In particular, they found that a "coherent destruction of tunneling" occurs at zeros of $J_0(2F\mu_{12}/\hbar\omega)$, where J_0 is the zeroth Bessel function, F the applied electric field, $\hbar\omega$ the photon energy, and μ_{12} the dipole moment between the two states. The basic underlying mechanism is the ability of a suitably chosen laser field to maintain the localization of an electron initially prepared in one side of the quartic double well. It was then demonstrated by Bavli and Metiu [3] that a laser field can even be used to localize an electron initially delocalized in both wells, provided the strength, frequency, and phase of the semi-infinite laser pulse are chosen properly. These results are not only of academic interest. Being able to control tunneling rates is of great potential use in as diverse fields as chemistry (steering chemical reactions) and optoelectronics (electro-optical switches).

A powerful tool for analyzing these effects is the Floquet-state formalism [4] which, by virtue of the periodicity of the Hamiltonian in time, enables us to define quasienergies of stationary states in the presence of a time-dependent electric field. It turns out that the Floquet states emerging from the almost degenerate two lowest states of the static quartic double well experience a crossing, or almost crossing, of their quasienergies exactly at the laser-field parameters where the coherent destruction of tunneling occurs. The interpretation follows that for the tunneling-induced level splitting between two static wells: The inverse of the energy splitting is a measure for the rate at which the two states communicate with each other or, in other words, for the tunneling rate. Hence, if the splitting tends to zero, the states localize and the tunneling rate will be correspondingly suppressed. This intriguing result has inspired a lot of work on driven two-state systems [5]. Among others, some groups have started addressing the question of dissipation [6], and a rather surprising result is that dissipation may not even be detrimental to the coherent destruction of tunneling, at least for some suitably chosen temperatures. Other work deals with the increased flexibility of control enjoyed by using two commensurate laser frequencies to drive a double well [7]. Nevertheless, apart from the quartic double well, only a few other systems have been looked at so far. For instance, Holthaus and Hone [8] have studied a finite superlattice embedded in a closed box and they also found a coherent destruction of tunneling for certain parameters of the laser field which they could explain by using the Floquet-state theory.

All these systems have in common that they are closed with respect to (electrical) particle exchange with their environment and hence that no dc current can flow. This means that the effect of coherent destruction of tunneling is only accessible to optical experiments. However, very recently, a similar effect termed "quenching of resonant transmission" was analytically studied in a harmonically driven double-barrier resonant tunneling diode [9]. (Weakly driven systems have, for instance, been considered in Ref. [10].) In this structure, the center quantum well is driven with $V_1\cos(\omega t)$, while the barrier and contact regions are assumed to be static. The driving potential generates additional sidebands at energies $E+n\hbar\omega$ in the transmission probability of traversing electrons, which can be interpretated as due to photon

absorbtion ($n > 0$) or emission ($n < 0$). A simultaneous strong quenching of the transmission probability in all sidebands is predicted at zeros of $J_n(\gamma V_1/\hbar\omega)$, where J_n is the Bessel function of the first kind with its index n depending on the energy E of the incoming electron, and γ is a structure-dependent parameter close to unity. The approach employed in Ref. [9] is an extension of the transfer-matrix method to harmonically driven systems and in part goes back to Büttiker and Landauer's discussion of the tunneling time through an oscillating barrier [11] and even much earlier work on microwave-driven superconducting tunneling diodes [12]. A quenching of the resonant transmission probability through a tunneling diode opens up exciting new possibilities, as now transport experiments can be used to probe the coherent destruction of tunneling. One has to bear in mind, though, that a major difference between open and closed systems seems to be that in the latter case at least two "interacting" Floquet states are necessary, while in an open system a single Floquet state is apparently enough to see the quenching. The origin of this difference is not fully understood yet. We are not aware of any transport experiment assessing the quenching effect in strongly driven open systems so far, but a number of experiments have been aimed at, for instance, the photon-assisted tunneling through quantum point contacts [13] or across quantum dots in the Coulomb-blockade regime [14–17].

The present paper extends previous work on driven double-barrier tunneling diodes [9], where the energy of the traversing electron had to match the energy $E_0+n\hbar\omega$ of the quantum-well resonance or one of its sidebands—the so-called resonant case—to arbitrary energies of the incoming electron. In Sec. II we briefly introduce the transfer-matrix approach to photon-assisted tunneling through a heterostructure, deferring a more detailed derivation to Appendixes A and B. In particular, we discuss the quenching of the transmission probability at certain parameters of the driving field for the nonresonant case, i.e., for incident electrons of energy $E \neq E_0 + n\hbar\omega$. In Sec. III we study the experimentally more readily accessible transmission probability integrated over all sidebands, while in Sec. IV the analysis of the escape time of the driven quantum-well resonance suggests that the quenching of the transmission probability does not correspond to a localization of a Floquet state as seen in closed systems. Finally, in Sec. V we present results on a double-barrier structure driven by oscillating potentials in the contact regions such that there is a phase difference of π between the left and right contact, which serves as a crude model for an *electric* driving field across the diode.

II. OSCILLATING QUANTUM WELL: NONRESONANT CASE

The transfer-matrix formalism is an often used tool for calculating the probability for an electron of energy E to traverse a quasi-one-dimensional heterostructure by means of tunneling [18]. The basic idea is to decompose the heterostructure into a number of smaller layers such that in each layer the Schrödinger equation can be solved analytically. For every layer, the most general solution can then be written as a linear combination of two linearly independent solutions $A\phi_1(z) + B\phi_2(z)$. To find a global solution across the entire heterostructure, one has to match these local solutions in each layer at their mutual boundaries, and the transfer matrices are simply a convenient way of expressing the rules for such a wave-function matching. In particular, the total transfer matrix relates the expansion coefficients A_l and B_l of the wave function on the left-hand side of the structure to those of the right-hand side,

$$\begin{pmatrix} A_r \\ B_r \end{pmatrix} = T^{l\to r} \begin{pmatrix} A_l \\ B_l \end{pmatrix}. \tag{1}$$

One particular advantage of the transfer-matrix approach is its modular structure: The total transfer matrix $T^{l\to r}$ is made up of the product of all the local transfer matrices for the individual layers in the heterostructure. Thus, when the properties of a single layer change, we only need to find the transfer matrix of this particular layer and plug it into the formula for $T^{l\to r}$. In the case of an oscillating quantum well, for instance, we have to calculate the transfer matrix in the presence of an additional modulating potential of the form $V_1(z)\cos(\omega t)$. A detailed derivation is given in Appendix A, and it is found that Eq. (1) has to be replaced by

$$\begin{pmatrix} A_r^n \\ B_r^n \end{pmatrix} = \sum_{n'=-\infty}^{\infty} T_{n,n'}^{l\to r} \begin{pmatrix} A_l^{n'} \\ B_l^{n'} \end{pmatrix}, \tag{2}$$

where n and n' denote the sidebands at $E + n\hbar\omega$ and $E + n'\hbar\omega$, respectively. The diagonal elements $T_{n,n}^{l\to r}$ are closely related to $T^{l\to r}$ in (1), while the off-diagonal elements $T_{n\neq n'}^{l\to r}$ describe the effects of $n-n'$ photon absorbtion respectively emission on the transmission probability of the electron, very similar in spirit to the theory of phonon-assisted tunneling [19]. For flatband conditions on both sides of the heterostructure, the wave functions $\phi_1(z)$ and $\phi_2(z)$ in the contacts are plane waves, and in this case the proper boundary conditions to describe an electron at energy E, incident from the left-hand side, are $A_l^n = \delta_{n,0}$ and $B_r^n = 0$. The transmission probability in sideband n is then defined as $T_n = \frac{k_r^n}{k_l^0}\frac{m_l}{m_r}|A_r^n/A_l^0|^2$, where k_r^n and k_l^0 are the wave vectors on the right- and left-hand sides in sidebands n and 0, respectively. One should note that this transmission probability is a *time-averaged* quantity and hence that the photon-assisted current as calculated in this paper is always the *dc response* to the ac driving field [20].

The model double-barrier structure used in the following is schematically shown in Fig. 1; two static barriers I and III enclose a quantum well II which is harmonically driven as $V_1\cos(\omega t)$. The parameters used are the same as in Ref. [9]: $m_{\mathrm{I,II,III}} = 0.067m_0$, $V_{\mathrm{I,III}} = 0.5$ eV, and $d_{\mathrm{QW}} = d_B = d = 5$ nm. In this section we analyze the nonresonant case, where the energy of the incoming electron neither matches the quantum-well resonance at E_0 nor one of the sidebands at $E_0 + n\hbar\omega$. The resonant

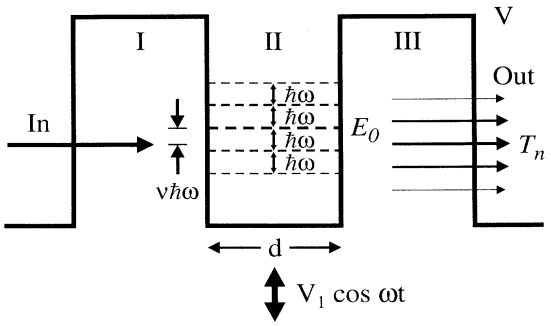

FIG. 1. Transmission channels through a driven double-barrier diode consisting of an oscillating quantum well sandwiched between two static barriers. As the incoming electron of energy E can pick up or lose photon quanta $\hbar\omega$, sidebands are formed in the transmission on the far side of the structure at energies $E + n\hbar\omega$. The amplitude of these sidebands is strongly affected by the driven quantum-well resonance at E_0.

case has been studied in Ref. [9], where it was shown that in a strongly driven system a simultaneous quenching of all transmission channels occurs at certain values $V_1/\hbar\omega > 1$.

A. Numerical results

The numerical analysis is much facilitated by the observation that to a very good approximation the transmission probability T_n is a function of $V_1/\hbar\omega$ only and hence using a single, fixed modulation frequency is sufficient. For the following discussion, we have chosen $\hbar\omega = 0.4$ meV, which is much smaller than both E_0 and $V_{\mathrm{I,III}} - E_0$, yet sufficiently large compared to the linewidth of the quantum-well resonance. For modulation frequencies smaller than this linewidth the scaling property will break down.

Figure 2 shows our results based on the transfer-matrix formalism for the transmission probability of an incoming electron $\hbar\omega/2$ below the quantum-well resonance at E_0. For better clarity, we have divided the various transmission channels into two classes: Panel (a) shows the transmission probability in sidebands where the electron has absorbed photon quanta when traversing the quantum well ($n \geq 0$), while in (b) the electron has emitted photon quanta ($n \leq 0$). At zero modulation amplitude V_1, only the center channel $n = 0$ is present, which is the common-sense result for a static double-barrier structure, whereas at large modulation amplitudes the transmission probability in the sidebands can be much higher than in the center band. The oscillatory structure as a function of $V_1/\hbar\omega$ is very similar to that found in the resonant case [9]. However, the simultaneous quenching of *all* transmission channels at certain values of $V_1/\hbar\omega$, as seen in the resonant case, has given way to a more complex behavior: The channels involving the absorbtion of photon quanta [Fig. 2(a)] quench separately from those involving the emission of photons [Fig. 2(b)]. The respective positions of quenching are indicated with arrows in Fig. 2 and the analysis shows that these positions can be described by

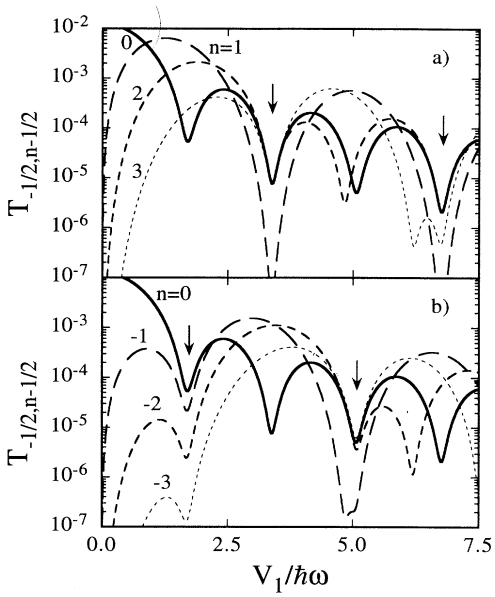

FIG. 2. Transmission probability $T_{-1/2,n-1/2}$ in sidebands n as a function of $V_1/\hbar\omega$ for an electron incident on a driven double-barrier diode $\hbar\omega/2$ below the quantum-well resonance, as calculated with the transfer-matrix method. The simultaneous quenching in the case of photon (a) absorption and (b) emission occurs at different values of $V_1/\hbar\omega$ (indicated by arrows).

the roots of $J_{\pm 1/2}(\gamma V_1/\hbar\omega)$, where $J_{\pm 1/2}$ is a fractional Bessel function and $\gamma = 0.93$ is the same parameter as determined in Ref. [9]. The plus sign refers to absorbtion and the minus sign to emission of photons. To support this interpretation, we also present results for the case of an incoming electron at energy $E_0 - \hbar\omega/4$ (see Fig. 3). In this case, the positions of quenching in (a) and (b) have moved closer to each other and now agree with

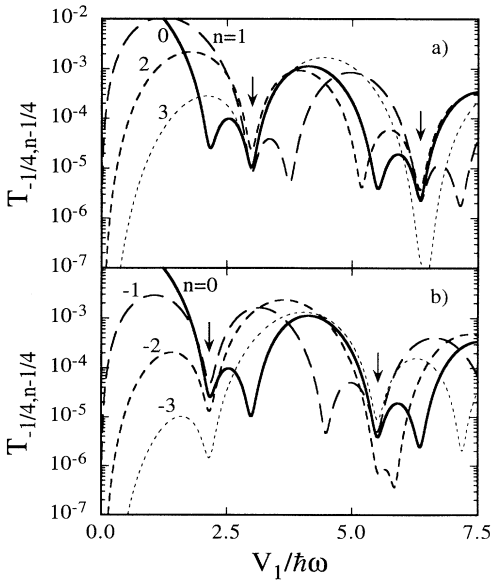

FIG. 3. Same as Fig. 2 for an incoming electron of energy $E = E_0 - \hbar\omega/4$. The difference in the positions of quenching in the (a) absorption and (b) emission channels, indicated with arrows, is now reduced.

the roots of $J_{\pm 1/4}(\gamma V_1/\hbar\omega)$. It is apparent from Figs. 2 and 3 that the resonant case is just a special case where the quenchings of the photon emission and absorbtion channels coincide.

B. Analytical results

In Appendix A it is shown that the wave function describing an electron incident at energy E together with its reflected and transmitted partial waves can be written as

$$\psi(E,z,t) = \psi^{\rm in}(z)\exp\left(-\tfrac{iEt}{\hbar}\right) + \sum_{n=-\infty}^{\infty}\psi_n(E,z,t)\exp\left(-\tfrac{i(E+n\hbar\omega)t}{\hbar}\right), \quad (3)$$

where $\psi_n(E,z,t)$ is the amplitude of sideband n. For the following, it is convenient to measure the energy E of the incoming electron with respect to the quantum-well resonance by introducing a dimensionless parameter ν such that $E = E_0 - \nu\hbar\omega$. The analytical analysis provided in Appendix B, which uses a similar approach to that given in Ref. [9], shows that to lowest order in $\hbar\omega$, but arbitrary order in $V_1/\hbar\omega$, the spectral weight $\|\psi_n\|^2$ of sideband n in the wave function (3) is proportional to

$$I_{-\nu,n-\nu}(\tfrac{V_1}{\hbar\omega}) \equiv \|\psi_n\|^2 \propto \begin{cases} \left|\frac{J_\nu(\gamma\frac{V_1}{\hbar\omega})}{J_{-\nu}(\gamma\frac{V_1}{\hbar\omega})}\right| \left|J_{n-\nu}(\gamma\tfrac{V_1}{\hbar\omega})\right|^2, & n>0 \\ \left|J_\nu(\gamma\tfrac{V_1}{\hbar\omega})J_{-\nu}(\gamma\tfrac{V_1}{\hbar\omega})\right|, & n=0 \\ \left|\frac{J_{-\nu}(\gamma\frac{V_1}{\hbar\omega})}{J_\nu(\gamma\frac{V_1}{\hbar\omega})}\right| \left|J_{\nu-n}(\gamma\tfrac{V_1}{\hbar\omega})\right|^2, & n<0, \end{cases} \quad (4)$$

where the parameter γ turns out to be the same as in the resonant case

$$\gamma = \frac{\pm k_{\rm II}^\nu d + \sinh(k_{\rm II}^\nu d)}{\pm k_{\rm II}^\nu d + \left[1 - \frac{m_{\rm I}}{m_{\rm II}}\left(\frac{k_{\rm II}^\nu}{k_{\rm I}^\nu}\right)^2\right]\sinh(k_{\rm II}^\nu d)} = \frac{\pm k_{\rm II}^\nu d + \sinh(k_{\rm II}^\nu d)}{\pm k_{\rm II}^\nu d \pm 2\frac{k_{\rm II}^\nu}{k_{\rm I}^\nu} + \left(1 - \frac{m_{\rm II}}{m_{\rm I}}\right)\sinh(k_{\rm II}^\nu d)}. \quad (5)$$

Here the plus sign is for odd and the minus sign for even quantum-well resonances.

A simple argument can now be used to calculate the relative transmission probabilities via different sidebands: In order to traverse the oscillating quantum well, an electron of energy $E = E_0 - \nu\hbar\omega$ first has to couple to the driven resonance in the quantum well. The probability for this to happen is proportional to the probability of finding the electron at energy E in the quantum well or, in other words, to the spectral weight $I_{-\nu,-\nu}(\frac{V_1}{\hbar\omega})$ of this energy in the scattering state. In the second step, the electron exits the quantum well via some sideband n, which again happens with a probability proportional to the spectral weight $I_{-\nu,n-\nu}(\frac{V_1}{\hbar\omega})$ of the sideband involved. Hence the transmission probability through an oscillating quantum well is proportional to the product of the spectral weights of both the incoming and the outgoing bands [21]

$$T_{-\nu,n-\nu}\left(\tfrac{V_1}{\hbar\omega}\right) \propto I_{-\nu,-\nu}\left(\tfrac{V_1}{\hbar\omega}\right) I_{-\nu,n-\nu}\left(\tfrac{V_1}{\hbar\omega}\right) \propto \begin{cases} \left|J_\nu\left(\gamma\frac{V_1}{\hbar\omega}\right)J_{n-\nu}\left(\gamma\frac{V_1}{\hbar\omega}\right)\right|^2, & n>0 \\ \left|J_\nu\left(\gamma\frac{V_1}{\hbar\omega}\right)J_{-\nu}\left(\gamma\frac{V_1}{\hbar\omega}\right)\right|^2, & n=0 \\ \left|J_{-\nu}\left(\gamma\frac{V_1}{\hbar\omega}\right)J_{\nu-n}\left(\gamma\frac{V_1}{\hbar\omega}\right)\right|^2, & n<0. \end{cases} \quad (6)$$

From (6) we see that all transmission channels in which photon quanta are absorbed ($n \geq 0$) quench simultaneously at zeros of $J_\nu(\gamma\frac{V_1}{\hbar\omega})$, while channels involving the emission of photon quanta ($n \leq 0$) do so at zeros of $J_{-\nu}(\gamma\frac{V_1}{\hbar\omega})$. Since for fractional ν the roots of $J_\nu(u)$ and $J_{-\nu}(u)$ do not coincide, a more complicated spectrum results as compared to the resonant case where ν is integer [22]. Essentially, the simultaneous quenching of all sidebands (marked with arrows in Figs. 3 and 4) is caused by the spectral weight $I_{-\nu,-\nu}(\frac{V_1}{\hbar\omega})$ of the incoming band tending to zero, which means that the incident electron cannot couple to the driven quantum-well resonance in the first place, and hence gets almost completely reflected. In addition to these simultaneous quenchings, individual quenchings of single channels, such as that of the $n = 1$ sideband in Fig. 3(a) at $V_1/\hbar\omega = 3.75$, happen when the spectral weight $I_{-\nu,n-\nu}(\frac{V_1}{\hbar\omega})$ of an *outgoing* sideband vanishes.

To illustrate the quality of our analytical solution, we present in Fig. 4 the results for the transmission probability for an electron at energy $E_0 - \hbar\omega/4$ based on Eq. (6), which has to be compared with the numerical transfer-matrix solution shown in Fig. 3, which takes into account higher orders in $\hbar\omega$. Using (5), the parameter γ was evaluated to $\gamma = 0.93$ and the data have been normalized with

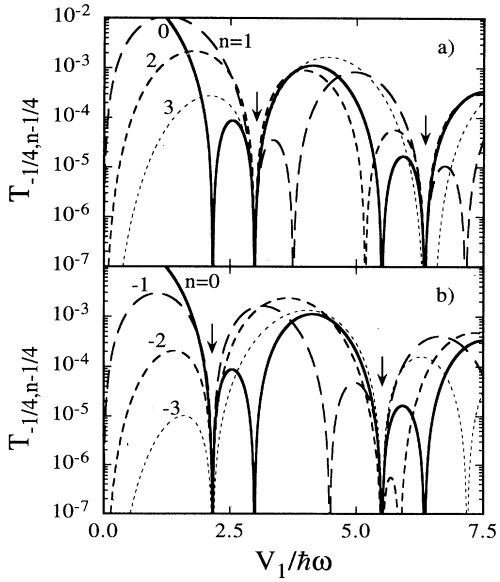

FIG. 4. Analytical results for the transmission probability $T_{-1/4,n-1/4} \propto I_{-1/4,-1/4} \times I_{-1/4,n-1/4}$. All parameters are the same as in Fig. 3.

reference to $T_{-\nu,-\nu}(0)$ of Fig. 3. The agreement found is excellent.

III. INTEGRATED TRANSMISSION PROBABILITIES

Essential to successfully measuring the quenching of the transmission probability of individual channels as a function of the driving amplitude V_1 is the ability to make energy-resolved measurements on the energy scale $\hbar\omega$. One way of achieving this is to add superlattices to the collector and emitter side of the heterostructure which then act as energy filters [23]. However, as these devices are fairly complicated, it would be interesting to see whether some fingerprints of the quenching could still be seen in somewhat simpler structures.

The simplest possible approach is to maintain the energy resolution at the incoming side, but to drop this requirement at the outgoing side of the heterostructure. In this case, we have to integrate over all transmission channels for fixed energy E of the incoming electron and the result is shown in Fig. 5 for various energies $E = E_0 - \nu\hbar\omega$. Although the quenchings of individual transmission channels have gone, the simultaneous quenching of all channels at particular values of $V_1/\hbar\omega$ is still clearly seen. The effect is most prominent close to the resonant case where ν is integer, but it can still be observed as far as $\hbar\omega/4$ off the resonance. As the energy of the incoming electron is lowered, the position of quenching moves towards higher modulation amplitudes V_1, but there seems to be a pinning at certain values of $V_1/\hbar\omega$. To inspect this more closely we have plotted in Fig. 6 the position of the first quenching of the total transmission probability T_ν of Fig. 5 as a function of $V_1/\hbar\omega$ (solid line). Indeed, pronounced plateaus are seen in the neighborhood of resonant transmission, i.e., around integer ν, where the position of the quenching depends only very weakly on the energy of the incoming electron. [What does change, however, is the degree of quenching (cf. the dashed curve in Fig. 5).] This means that the requirements on the energy resolution at the input side are not as severe as one might first think. In particular, the quenching effect should still be visible for

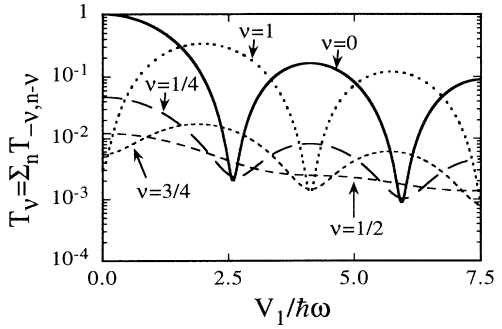

FIG. 5. Total transmission probability $T_\nu = \sum_n T_{-\nu,n-\nu}$ as a function of $V_1/\hbar\omega$ for various energies of the incoming electron $E = E_0 - \nu\hbar\omega$. Quenching is most pronounced for resonant transmission (ν integer).

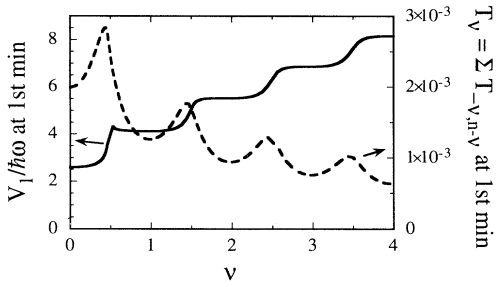

FIG. 6. Position (solid line) and value (dotted line) of the first quenching of the total transmission probability T_ν of Fig. 5 as a function of $V_1/\hbar\omega$. Pronounced plateaus are seen in the neighborhood of resonant transmission (ν integer).

an incoming electron distribution with an energy broadening of up to about $\hbar\omega/4$.

One possible, albeit certainly difficult, way to achieve a sufficiently monochromatic electron beam at the input side is to use only a weak dc bias across the diode $V_{sd} < \hbar\omega$ and low temperatures $k_BT \ll \hbar\omega$. In this case, only the electrons at the Fermi energy contribute to the net current and the dc current response, i.e., the photon-assisted current, will be proportional to T_ν. Another approach would be to engineer the conduction-band edge in the emitter by means of a clever doping profile to be just below the Fermi energy.

IV. ESCAPE TIME OF A DRIVEN RESONANCE

A characteristic fingerprint of the coherent destruction of tunneling in closed systems such as the quartic double well is a strong localization of the states at these particular parameters of the laser field. It is therefore interesting to see whether a similar localization occurs in the driven double-barrier structure as well. To this end we used the complex-energy formalism [18] to calculate the lifetime of the quantum-well resonance as a function of the amplitude of the driving field. It turns out that the effect of the driving field on the lifetime is extremely small [24]. In the example studied above the lifetime decreased monotonically from 14.743 ps for a static quantum well to about 14.738 ps at $V_1/\hbar\omega = 7.5$. In particular, the quenching of the transmission probability as seen in Figs. 2 and 3 does not show up as a corresponding resonance in the lifetime. We therefore conclude that in our system the quenching or coherent destruction of tunneling is *not* accompanied by a localization of the Floquet state as seen, for instance, in a closed quartic double well.

V. OSCILLATING ELECTRIC FIELD ACROSS A DOUBLE-BARRIER TUNNELING DIODE

The scenario where the center quantum well of the tunneling diode is driven as $V_1\cos(\omega t)$ while the barrier and contact regions remain largely unaffected may be realized by electrostatic gates close to the quantum-well layer. A

different situation arises when an ac bias is applied across the tunneling diode or when the diode is irradiated with a laser field, which may be better described by a driving electric field $F(z)\cos(\omega t)$ across the diode instead of an oscillating flat potential in the center quantum well. To tackle this case within the framework of the transfer-matrix method, we have to divide the corresponding driving potential $V_1(z,t) = e\int_0^z dz' F(z')\cos(\omega t)$ into many steps such that $V_1(z)$ can be assumed to be constant within each step.

As each step requires the computation of a rather large transfer matrix, we shall study only a very crude model for a driving electric field. As in Fig. 1 we divide the structure into five layers, with the contact regions now oscillating in antiphase as $\pm V_1\cos(\omega t)$. The barrier layers experience only a reduced driving potential $\pm gV_1\cos(\omega t)$ with $g < 1$ depending on the geometry of the diode, while the central quantum well remains static. In Fig. 7 we present results for the probability of an electron at energy E_0 to resonantly traverse the electric-field driven tunneling diode. Again, a simultaneous quenching is seen at particular parameters $\{V_1, \omega\}$ of the driving field and an analysis in terms of zeros of Bessel functions shows that these quenchings can be described by zeros of $J_n(\gamma V_1/\hbar\omega)$, where γ=1.000 26 ± 0.000 22.

In general, for asymmetrically driven systems, there will be three, instead of two, relevant field parameters V_1^l, V_1^r, and ω, where V_1^l is the driving potential between the left-hand region and the quantum well and V_1^r that between the quantum well and the right-hand region [25]. Correspondingly, there will be two different series of quenching, one associated with $V_1^l/\hbar\omega$ and the other with $V_1^r/\hbar\omega$. In the present symmetric case, though, we have $V_1^l = V_1^r = V_1$ and these two series coincide. Nevertheless, a residual interference between them can still be seen in Fig. 7 as a doublet fine structure in the central band at $V_1/\hbar\omega \approx 2.4$ and 5.5. This interpretation is further supported by the observation that in Fig. 7 the quenching of the sidebands is much more pronounced as compared to Figs. 2 and 3, and also Fig. 4 of Ref. [9], suggesting that as the V_1^l and V_1^r series of quenching collapse into a single series, their strengths roughly multiply.

These characteristics persist for electrons incident at

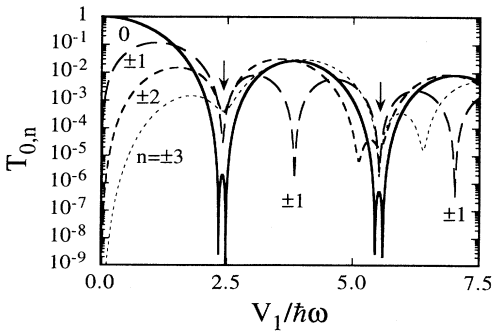

FIG. 7. Transmission probability $T_{0,n}$ in sidebands n as a function of $V_1/\hbar\omega$ for an electron of energy E_0 resonantly incident on a double-barrier diode driven by an *electric field*, which is simulated by a static central quantum well and the potential in the emitter oscillating in antiphase to the collector potential $[V_C(t) = -V_E(t) = V_1\cos(\omega t)]$.

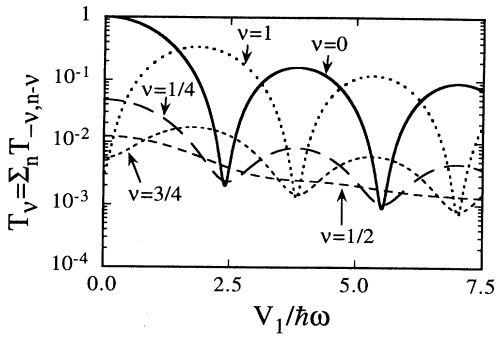

FIG. 8. Total transmission probability $T_\nu = \sum_n T_{-\nu,n-\nu}$ as in Fig. 5, but now for a diode driven by an electric field across the double-barrier structure. Even though the driving method is rather different, the resulting T_ν is virtually the same after accounting for the slightly different γ values.

other energies $E = E_0 - \nu\hbar\omega$, but again, as in the case of the oscillating-quantum-well tunneling diode studied above, for noninteger ν the simultaneous quenching of all sidebands is lost. Moreover, for noninteger ν we were unable to interpret the positions of quenchings as zeros of Bessel functions. Nonetheless, the total transmission probability, defined as the sum over all transmission channels, shows a striking similarity to that of the oscillating-quantum-well tunneling diode; Figs. 8 and 5 are virtually identical if we account for the slightly different scaling factor γ of the driving amplitude.

VI. CONCLUSIONS

In conclusion, we have studied photon-assisted electron transport through a driven double-barrier resonant tunneling diode within the framework of the transfer-matrix formalism. In the first example, a driving potential $V_1\cos(\omega t)$ acting on the central quantum well of the tunneling diode caused additional sidebands at energies $E + n\hbar\omega$ to open up in the transmission probability of traversing electrons due to photon absorbtion $(n > 0)$ and emission $(n < 0)$. A strong quenching of these channels was found at certain parameters $\{V_1, \omega\}$ of the driving potential. In particular, transmission channels requiring photon absorbtion quench simultaneously at zeros of $J_\nu(\gamma\frac{V_1}{\hbar\omega})$, where J_ν is a fractional Bessel function, while channels involving photon emission do so at zeros of $J_{-\nu}(\gamma\frac{V_1}{\hbar\omega})$. Here $-\nu\hbar\omega = E - E_0$ is the energy of the electron relative to the quantum-well resonance and the parameter $\gamma \approx 1$ depends on the structure of the diode. A simultaneous quenching of *all* channels is only seen for integer ν, i.e., for the case of resonant transmission. These results can be understood in terms of vanishing amplitudes in the spectral decomposition of the wave function of the scattering state at the energy of the incident electron.

The second example considered is a simple model for a double-barrier tunneling diode driven by an electric field $F(z)\cos(\omega t)$ across the diode, which is a situation typical for diodes irradiated by a laser field. For the symmetric

case studied here, the parameter relevant for quenching is the ratio of the potential drop between emitter and quantum well, $V_1 = e\int dzF(z)$, to the photon energy $\hbar\omega$ of the driving field. For the case of resonant transmission, we again find that the quenching can be described by zeros of integer Bessel functions $J_n(\gamma V_1/\hbar\omega)$, with $\gamma \approx 1$ as structural parameter, while the nonresonant case is not well understood yet. Interestingly, even though the driving mechanisms in the two examples studied here are rather different, we find that after accounting for the slightly different structural parameters γ, the sum over all transmission channels looks almost identical in both examples.

In order to see the quenching effect experimentally, one would need electrons incident onto the double barrier of the tunneling diode with an energy distribution better than $\hbar\omega/4$, which may be realized with energy filters such as superlattices. Alternatively, such a filtering could be achieved at very low temperatures $k_BT \ll \hbar\omega$ by restricting the dc bias across the diode to a range $V_{sd} < \hbar\omega$. In both cases, the photon-assisted current is the dc current in response to the ac driving field. The problem of finding a suitable range of experimentally accessible parameters should be eased somewhat by the fact that the position of quenching scales linearly with the photon energy of the driving field.

Our results may be useful for getting a better understanding of a related effect, termed "coherent destruction of tunneling," which occurs in driven closed systems such as, for instance, a harmonically driven quartic double well. In particular, our work shows that this effect can be studied not only using optical techniques, but also in transport experiments. The main difference to previous work on the coherent destruction of tunneling is the fact that in the latter case two almost degenerate Floquet states are necessary in order to observe the effect, while in the driven double-barrier tunneling diode studied here a single Floquet state is sufficient. Moreover, this Floquet state does not localize at quenching—indicated by the absence of any resonance in its lifetime—which is also in contrast to results found for closed systems. We attribute these differences to the fact that in a closed double-well system the two Floquet states probe each other, whereas in our system an external electron beam of adjustable energy is used for probing the spectral decomposition of a single Floquet state.

Note added in proof. M. Holthaus pointed out to me the important work of D. H. Dunlap and V. M. Kenkre on the dynamic localization of a charged particle moving on a tight-binding lattice under the influence of an electric field [Phys. Rev. B **34**, 3625 (1986)]. The "dynamical localization" they discussed is very similar to the "coherent destruction of tunneling" in a double quantum well.

ACKNOWLEDGMENTS

I have benefited from many stimulating discussions with Jeremy Allam, Albert Heberle, David Williams, Bruce Alphenaar, Ken Ogawa, and Kazuo Nakazato, which are gratefully acknowledged.

APPENDIX A: DEFINITION OF TRANSFER MATRICES

In this appendix, the standard transfer-matrix approach is reformulated to account for a harmonically oscillating potential in a quasi-one-dimensional time-dependent Hamiltonian of the form [26]

$$H(z,t) = H_0(z) + V_1(z)\cos(\omega t) = -\frac{\hbar^2}{2}\frac{\partial}{\partial z}\frac{1}{m(z)}\frac{\partial}{\partial z} + V(z) + V_1(z)\cos(\omega t). \quad \text{(A1)}$$

Here $V(z)$, $V_1(z)$, and $m(z)$ are step functions, i.e., piecewise constant. The notation used follows Refs. [9] and [18].

For a spatially uniform modulation amplitude $V_1(z) = V_1$, a particular solution to the corresponding time-dependent Schrödinger equation $i\hbar\frac{\partial}{\partial t}\psi(z,t) = H(z,t)\psi(z,t)$ is [12]

$$\psi(z,t) = \psi_0(z)\exp\left(-\tfrac{iEt}{\hbar}\right)\exp\left[-i\tfrac{V_1}{\hbar\omega}\sin(\omega t)\right] = \psi_0(z)\exp\left(-\tfrac{iEt}{\hbar}\right)\sum_{n=-\infty}^{\infty} J_n\left(\tfrac{V_1}{\hbar\omega}\right)\exp(-in\omega t), \quad \text{(A2)}$$

where J_n is the Bessel function of the first kind and $\psi_0(z)$ solves the time-independent Schrödinger equation $H_0(z)\psi_0(z) = E\psi_0(z)$. There are two points about Eq. (A2) which we would like to stress: (i) Though valid for $V_1(z) = \text{const}$ only, it holds for *arbitrary* potentials $V(z)$, and (ii) as this wave function solves the *time-dependent* Schrödinger equation, it does not possess a single eigenenergy, but rather can be characterized by a whole series of evenly spaced energies $\{E + n\hbar\omega \,|\, n \text{ integer}\}$. This latter observation means that if we replace E in Eq. (A2) by $E + l\hbar\omega$, the resulting wave function can still be characterized by the same energy ladder $\{E + n\hbar\omega \,|\, n \text{ integer}\}$ [27]. Hence the most general wave function for a given energy ladder is a linear combination of particular solutions of the form (A2) at energies $E + l\hbar\omega$,

$$\psi(E,z,t) = \sum_{l=-\infty}^{\infty}\psi_l(z)\exp\left(-\tfrac{i(E+l\hbar\omega)t}{\hbar}\right) \times \exp\left[-i\tfrac{V_1}{\hbar\omega}\sin(\omega t)\right] = \exp\left(-\tfrac{iEt}{\hbar}\right)\sum_{l=-\infty}^{\infty}\psi_l(z) \times \sum_{n=-\infty}^{\infty} J_n\left(\tfrac{V_1}{\hbar\omega}\right)\exp[-i(n+l)\omega t]. \quad \text{(A3)}$$

Here we have defined $\psi_l(z)$ to be a solution of $H_0(z)\psi_l(z) = (E + l\hbar\omega)\psi_l(z)$. The index l is usually referred to as the sideband index relative to the $l = 0$ center band at energy E. Note also that the normalization of the coefficients $\psi_l(z)$, i.e., the intensity of the sidebands, are parameters which have to be determined from the boundary conditions at energies $E + l\hbar\omega$ and

the normalization of $\psi(E,z,t)$.

In order to set up a transfer-matrix description, we next approximate the potential $V(z)+V_1(z)\cos(\omega t)$ by a series of small steps of layers I, II, III, etc. in which $V(z)$, $V_1(z)$, and the effective mass $m(z)$ can be assumed to be constant. The accuracy of this approximation can be easily controlled by increasing the number of layers. Then, in any layer, the parameter functions $\psi_l(z)$ of each sideband are simply linear combinations of plane waves $\psi_l(z) = A^l\exp(k^l z) + B^l\exp(-k^l z)$ with wave vector $\hbar k^l = \sqrt{2m(V-E-l\hbar\omega)}$. (Note that, in order to unify the notation, in our definition the wave vector can be real or imaginary, thus describing propagating waves as well as decaying and diverging solutions. This is different from the approach taken in Ref. [9].)

Now let the modulation amplitude V_1 vanish in layer I. Then, from Eq. (A3), the most general wave function for a given energy ladder reads

$$\psi_{\rm I}(E,z,t) = \sum_{l=-\infty}^{\infty}\left[A_{\rm I}^l\exp(k_{\rm I}^l z) + B_{\rm I}^l\exp(-k_{\rm I}^l z)\right] \times\exp\left(-\tfrac{i(E+l\hbar\omega)t}{\hbar}\right), \tag{A4}$$

with the wave vector of each sideband l given by $\hbar k_{\rm I}^l = \sqrt{2m_{\rm I}(V_{\rm I}-E-l\hbar\omega)}$. On the other hand, if the modulation amplitude V_1 is finite in layer II, we find, from Eq. (A3),

$$\psi_{\rm II}(E,z,t) = \sum_{l=-\infty}^{\infty}\left[A_{\rm II}^l\exp(k_{\rm II}^l z) + B_{\rm II}^l\exp(-k_{\rm II}^l z)\right] \times\sum_{n=-\infty}^{\infty} J_n\left(\tfrac{V_1}{\hbar\omega}\right)\exp\left[-\tfrac{i[E+(l+n)\hbar\omega]t}{\hbar}\right], \tag{A5}$$

where $\hbar k_{\rm II}^l = \sqrt{2m_{\rm II}(V_{\rm II}-E-l\hbar\omega)}$.

When matching the wave functions in layers I and II at their common interface $z=z_i$, the boundary condition in the effective-mass approximation is that the wave function and its flux have to be continuous,

$$\psi_{\rm I}(E,z_i,t) = \psi_{\rm II}(E,z_i,t),$$
$$\frac{1}{m_{\rm I}}\frac{\partial}{\partial z}\psi_{\rm I}(E,z,t)\Big|_{z=z_i} = \frac{1}{m_{\rm II}}\frac{\partial}{\partial z}\psi_{\rm II}(E,z,t)\Big|_{z=z_i}. \tag{A6}$$

As this boundary condition has to hold at every instant in time, the coefficients of the energy phase factors must already satisfy this boundary condition, leading to an infinite system of algebraic equations

$$A_{\rm I}^n\exp(k_{\rm I}^n z_i) + B_{\rm I}^n\exp(-k_{\rm I}^n z_i) = \sum_{l=-\infty}^{\infty}\left[A_{\rm II}^l\exp(k_{\rm II}^l z_i) + B_{\rm II}^l\exp(-k_{\rm II}^l z_i)\right] J_{n-l}\left(\tfrac{V_1}{\hbar\omega}\right) \tag{A7}$$

$$\frac{k_{\rm I}^n}{m_{\rm I}}\left[A_{\rm I}^n\exp(k_{\rm I}^n z_i) - B_{\rm I}^n\exp(-k_{\rm I}^n z_i)\right] = \sum_{l=-\infty}^{\infty}\frac{k_{\rm II}^l}{m_{\rm II}}\left[A_{\rm II}^l\exp(k_{\rm II}^l z_i) - B_{\rm II}^l\exp(-k_{\rm II}^l z_i)\right] \times J_{n-l}\left(\tfrac{V_1}{\hbar\omega}\right)$$

This can be rewritten in a more compact matrix form

$$\sum_{l=-\infty}^{\infty} T^{\rm I}_{z_i;n,l}\begin{pmatrix}A_{\rm I}^l\\ B_{\rm I}^l\end{pmatrix} = \sum_{l=-\infty}^{\infty} T^{\rm II}_{z_i;n,l}\begin{pmatrix}A_{\rm II}^l\\ B_{\rm II}^l\end{pmatrix}, \tag{A8}$$

with

$$T^{\rm I}_{z_i;n,l} = \delta_{n,l}\begin{pmatrix}\exp(k_{\rm I}^n z_i) & \exp(-k_{\rm I}^n z_i)\\ \frac{k_{\rm I}^n}{m_{\rm I}}\exp(k_{\rm I}^n z_i) & -\frac{k_{\rm I}^n}{m_{\rm I}}\exp(-k_{\rm I}^n z_i)\end{pmatrix} \tag{A9}$$

and

$$T^{\rm II}_{z_i;n,l} = J_{n-l}\left(\tfrac{V_1}{\hbar\omega}\right) \times\begin{pmatrix}\exp(k_{\rm II}^l z_i) & \exp(-k_{\rm II}^l z_i)\\ \frac{k_{\rm II}^l}{m_{\rm II}}\exp(k_{\rm II}^l z_i) & -\frac{k_{\rm II}^l}{m_{\rm II}}\exp(-k_{\rm II}^l z_i)\end{pmatrix}. \tag{A10}$$

With the identity $\sum_{l=-\infty}^{\infty} J_{n-l}(u)J_{n'-l}(u) = \delta_{n,n'}$, Eq. (A10) can be easily inverted to give

$$\left(T^{\rm II}_{z_i}\right)^{-1}_{l,n} = \frac{1}{2}J_{n-l}\left(\tfrac{V_1}{\hbar\omega}\right) \times\begin{pmatrix}\exp(-k_{\rm II}^l z_i) & \frac{m_{\rm II}}{k_{\rm II}^l}\exp(-k_{\rm II}^l z_i)\\ \exp(k_{\rm II}^l z_i) & -\frac{m_{\rm II}}{k_{\rm II}^l}\exp(k_{\rm II}^l z_i)\end{pmatrix}. \tag{A11}$$

The transfer matrix across layer II from z_1 to z_2 is then finally given by

$$T^{z_1\to z_2}_{n,n'} = \sum_{l=-\infty}^{\infty} T^{\rm II}_{z_2;n,l}\left(T^{\rm II}_{z_1}\right)^{-1}_{l,n'} = \sum_{l=-\infty}^{\infty} J_{n-l}\left(\tfrac{V_1}{\hbar\omega}\right)J_{n'-l}\left(\tfrac{V_1}{\hbar\omega}\right) \times\begin{pmatrix}\cosh(k_{\rm II}^l d) & \frac{m_{\rm II}}{k_{\rm II}^l}\sinh(k_{\rm II}^l d)\\ \frac{k_{\rm II}^l}{m_{\rm II}}\sinh(k_{\rm II}^l d) & \cosh(k_{\rm II}^l d)\end{pmatrix}, \tag{A12}$$

with $d = z_2 - z_1$ being the width of layer II. For vanishing modulation amplitude $V_1 \longrightarrow 0$, (A12) reduces to the familiar expression (A13) of Ref. [18]. For finite modulation amplitude, we first expand the wave vector $\hbar k_{\rm II}^l = \sqrt{2m_{\rm II}(V_{\rm II}-E-l\hbar\omega)}$ in a power series of l and then evaluate the resulting sums of the general form $\sum_{l=-\infty}^{\infty} l^j J_{n-l}(u)J_{n'-l}(u)$ exactly by recursion [28]. To lowest order we find

$$\sum_{l=-\infty}^{\infty} J_{n-l}(u)J_{n'-l}(u) = \delta_{n,n'},$$

$$\sum_{l=-\infty}^{\infty} l J_{n-l}(u)J_{n'-l}(u) = n\delta_{n,n'} - \frac{u}{2}\left(\delta_{n,n'+1} + \delta_{n,n'-1}\right),$$

$$\sum_{l=-\infty}^{\infty} l^2 J_{n-l}(u)J_{n'-l}(u) = \left(n^2+\frac{u^2}{2}\right)\delta_{n,n'} - u\left(n-\frac{1}{2}\right)\delta_{n,n'+1} - u\left(n+\frac{1}{2}\right)\delta_{n,n'-1} + \frac{u^2}{4}\left(\delta_{n,n'+2} + \delta_{n,n'-2}\right). \tag{A13}$$

This perturbation series usually converges very quickly as it depends only on $\hbar\omega$ being much smaller than V and $E-V$ (in order for the $k_{\rm II}^l$ expansion to converge quickly). Its main virtue is that it is *not* an expansion in $V_1/\hbar\omega$, but holds for *arbitrary* ratios $V_1/\hbar\omega$, and can thus be used to study strongly driven systems. Another issue is the fact that the transfer matrix has an infinite rank and thus needs to be truncated for numerical computation. The number of sidebands included depends on their spectral weight in the wave function, i.e., on $V_1/\hbar\omega$. In our case we set the cutoff weight to 10^{-15} and found $n_{\max}=31$ to be sufficient up to $\gamma V_1/\hbar\omega = 7.5$. Finally, we note that a static electric field can be easily included in our derivation of a transfer matrix by using Airy functions [18] instead of plane waves as a basis set in each layer.

APPENDIX B: NONRESONANT TRANSMISSION THROUGH A STRONGLY DRIVEN QUANTUM WELL

In this appendix we derive an analytical expression for the transmission probability for an electron of arbitrary energy E to traverse an oscillating quantum well. The more limited case where the energy of the incoming electron has to match one of the sidebands of the quantum-well resonance has already been established in Ref. [9].

As in Ref. [9] we consider a quantum well consisting of two static barrier regions I and III and a central driven quantum-well region II (see Fig. 1). We use the boundary conditions (A7) at the interfaces $x=0$ and $x=d$ of the quantum well to eliminate the coefficients $A_{\rm II}^n$, and $B_{\rm II}^n$, thereby arriving at an infinite set of algebraic equations for the remaining coefficients $A_{\rm I}^n$, $B_{\rm I}^n$, $A_{\rm III}^n$, and $B_{\rm III}^n$ of the barrier regions

$$\sum_{n=-\infty}^{\infty}\left[\alpha^{\rm I}(n,l)A_{\rm I}^n+\beta^{\rm I}(n,l)B_{\rm I}^n\right]J_{n-l}\left(\tfrac{V_1}{\hbar\omega}\right)$$
$$=\sum_{n=-\infty}^{\infty}\left[\alpha^{\rm III}(n,l)A_{\rm III}^n\exp(k_{\rm III}^n d)+\beta^{\rm III}(n,l)B_{\rm III}^n\exp(-k_{\rm III}^n d)\right]J_{n-l}\left(\tfrac{V_1}{\hbar\omega}\right)\exp(-k_{\rm II}^l d), \tag{B1}$$

$$\sum_{n=-\infty}^{\infty}\left[\beta^{\rm I}(n,l)A_{\rm I}^n+\alpha^{\rm I}(n,l)B_{\rm I}^n\right]J_{n-l}\left(\tfrac{V_1}{\hbar\omega}\right)$$
$$=\sum_{n=-\infty}^{\infty}\left[\beta^{\rm III}(n,l)A_{\rm III}^n\exp(k_{\rm III}^n d)+\alpha^{\rm III}(n,l)B_{\rm III}^n\exp(-k_{\rm III}^n d)\right]J_{n-l}\left(\tfrac{V_1}{\hbar\omega}\right)\exp(k_{\rm II}^l d).$$

Here we have defined $\alpha^{\rm I,III}(n,l)=1+\frac{m_{\rm II}}{k_{\rm II}^l}\frac{k_{\rm I,III}^n}{m_{\rm I,III}}$ and $\beta^{\rm I,III}(n,l)=1-\frac{m_{\rm II}}{k_{\rm II}^l}\frac{k_{\rm I,III}^n}{m_{\rm I,III}}$. By adding and subtracting these two sets of equations and summing over l we find, again with the help of $\sum_{l=-\infty}^{\infty}J_{n-l}(u)J_{n'-l}(u)=\delta_{n,n'}$,

$$A_{\rm I}^{n'}+B_{\rm I}^{n'}=\sum_{l,n=-\infty}^{\infty}\Bigg\{\Bigg[\cosh(k_{\rm II}^l d)-\frac{k_{\rm III}^n}{m_{\rm III}}\frac{m_{\rm II}}{k_{\rm II}^l}\sinh(k_{\rm II}^l d)\Bigg]A_{\rm III}^n\exp(k_{\rm III}^n d)+\Bigg[\cosh(k_{\rm II}^l d)+\frac{k_{\rm III}^n}{m_{\rm III}}\frac{m_{\rm II}}{k_{\rm II}^l}\sinh(k_{\rm II}^l d)\Bigg]\times B_{\rm III}^n\exp(-k_{\rm III}^n d)\Bigg\}J_{n-l}\left(\tfrac{V_1}{\hbar\omega}\right)J_{n'-l}\left(\tfrac{V_1}{\hbar\omega}\right), \tag{B2}$$

$$A_{\rm I}^{n'}-B_{\rm I}^{n'}=-\frac{m_{\rm I}}{k_{\rm I}^{n'}}\sum_{l,n=-\infty}^{\infty}\Bigg\{\Bigg[\frac{k_{\rm II}^l}{m_{\rm II}}\sinh(k_{\rm II}^l d)-\frac{k_{\rm III}^n}{m_{\rm III}}\cosh(k_{\rm II}^l d)\Bigg]A_{\rm III}^n\exp(k_{\rm III}^n d)+\Bigg[\frac{k_{\rm II}^l}{m_{\rm II}}\sinh(k_{\rm II}^l d)+\frac{k_{\rm III}^n}{m_{\rm III}}\cosh(k_{\rm II}^l d)\Bigg]\times B_{\rm III}^n\exp(-k_{\rm III}^n d)\Bigg\}J_{n-l}\left(\tfrac{V_1}{\hbar\omega}\right)J_{n'-l}\left(\tfrac{V_1}{\hbar\omega}\right).$$

The integers n, n', and l employed here refer to the energy E used in Eqs. (A4) and (A5) which has not been specified yet. It is now convenient to specify this energy to be that of the incoming electron, so that $n=0$ refers to the center band where the energy of the traversing electron remains unchanged [29]. In order to find an analytical solution to (B2), we expand all wave vectors to lowest order in $\hbar\omega$ about the wave vector of the quantum well resonance at energy E_0. This expansion can be conveniently parametrized by a parameter ν defined by $E_0=E+\nu\hbar\omega$. To keep things simple, we further assume in the following a symmetric quantum well having $V_{\rm I}=V_{\rm III}$ and $m_{\rm I}=m_{\rm III}$. A calculation similar to that in Ref. [9] then shows that the resulting system of equations can be solved by the ansatz [30]

$$\left.\begin{matrix}A_{\rm III}^n\exp(k_{\rm III}^n d),\\ B_{\rm III}^n\exp(-k_{\rm III}^n d)\end{matrix}\right\}\propto\begin{cases}\sqrt{\frac{J_\nu(\gamma\frac{V_1}{\hbar\omega})}{J_{-\nu}(-\gamma\frac{V_1}{\hbar\omega})}}J_{n-\nu}(\gamma\frac{V_1}{\hbar\omega}), & n>0\\ \sqrt{J_\nu(\gamma\frac{V_1}{\hbar\omega})J_{-\nu}(-\gamma\frac{V_1}{\hbar\omega})}, & n=0\\ \sqrt{\frac{J_{-\nu}(-\gamma\frac{V_1}{\hbar\omega})}{J_\nu(\gamma\frac{V_1}{\hbar\omega})}}J_{\nu-n}(-\gamma\frac{V_1}{\hbar\omega}), & n<0,\end{cases} \tag{B3}$$

where the parameter γ turns out to be different for the A^n and B^n series of coefficients

$$\gamma_{A,B} = \frac{C_{A,B}k_{\rm II}^{\nu}d + \sinh(k_{\rm II}^{\nu}d)}{C_{A,B}k_{\rm II}^{\nu}d + \left[1 - \frac{m_{\rm I}}{m_{\rm II}}\left(\frac{k_{\rm II}^{\nu}}{k_{\rm I}^{\nu}}\right)^2\right]\sinh(k_{\rm II}^{\nu}d)} = \frac{C_{A,B}k_{\rm II}^{\nu}d + \sinh(k_{\rm II}^{\nu}d)}{C_{A,B}k_{\rm II}^{\nu}d \pm 2\frac{k_{\rm II}^{\nu}}{k_{\rm I}^{\nu}} + \left(1 - \frac{m_{\rm II}}{m_{\rm I}}\right)\sinh(k_{\rm II}^{\nu}d)}. \quad \text{(B4)}$$

The constants $C_{A,B}$ are given by

$$C_A = \pm 1 + 2\frac{k_{\rm II}^{\nu}}{k_{\rm I}^{\nu}}\frac{m_{\rm I}}{m_{\rm II}}\sinh(k_{\rm II}^{\nu}d), \quad C_B = \pm 1, \quad \text{(B5)}$$

where the plus sign is for odd quantum-well resonances and the minus sign for even resonances.

The transmission probability $T_{-\nu,n-\nu}$ through channel n is proportional to the product of the spectral weights $I_n \propto |A_{\rm III}^n|^2 + |B_{\rm III}^n|^2$ of the incoming ($n_{\rm in} = 0$) and outgoing ($n_{\rm out} = n$) sidebands as discussed in [9]. If either the $A^n(z)$ or the $B^n(z)$ series of coefficients is dominant (as is the case for a strongly bound quantum-well resonance), (B3) leads to

$$T_{-\nu,n-\nu}\left(\frac{V_1}{\hbar\omega}\right) \propto \begin{cases} \left|J_\nu\left(\gamma\frac{V_1}{\hbar\omega}\right)J_{n-\nu}\left(\gamma\frac{V_1}{\hbar\omega}\right)\right|^2, & n > 0 \\ \left|J_\nu\left(\gamma\frac{V_1}{\hbar\omega}\right)J_{-\nu}\left(\gamma\frac{V_1}{\hbar\omega}\right)\right|^2, & n = 0 \\ \left|J_{-\nu}\left(\gamma\frac{V_1}{\hbar\omega}\right)J_{\nu-n}\left(\gamma\frac{V_1}{\hbar\omega}\right)\right|^2, & n < 0 \end{cases} \quad \text{(B6)}$$

with $\gamma = \gamma_A$ or $\gamma = \gamma_B$, respectively. [Here we have utilized that $|J_\nu(u)| = |J_\nu(-u)|$ holds for arbitrary real ν.] It should be noted that according to (B3) the sideband amplitudes diverge at zeros of the Bessel functions, while the final result for the transmission probability (B6) does not. This singularity of the sideband amplitudes is removed if higher orders of $\hbar\omega$ are taken into account. Finally, the remaining proportionality factor in (B6) can be determined for noninteger ν from the static case $T_{-\nu,n-\nu}(0) = \delta_{n,0}T_{-\nu,-\nu}(0)$.

Again, we point out that the relevant parameter used in the perturbation expansion leading to Eq. (B6) is $\hbar\omega$ and *not* $V_1/\hbar\omega$. The results are thus suitable for strongly driven systems.

[1] P. Holmes, Philos. Trans. R. Soc. London, Ser. A **292**, 419 (1979); B.A. Huberman and J.P. Crutchfield, Phys. Rev. Lett. **43**, 1743 (1979); Y. Ueda, J. Stat. Phys. **20**, 181 (1979); Ann. N.Y. Acad. Sci. **357**, 422 (1980).

[2] F. Großmann, T. Dittrich, and P. Hänggi, Physica B **175**, 293 (1991); F. Großmann, P. Jung, T. Dittrich, and P. Hänggi, Z. Phys. B **84**, 315 (1991); F. Großmann, T. Dittrich, P. Jung, and P. Hänggi, Phys. Rev. Lett. **67**, 516 (1991).

[3] R. Bavli and H. Metiu, Phys. Rev. Lett. **69**, 1986 (1992); Phys. Rev. A **47**, 3299 (1993).

[4] J.H. Shirley, Phys. Rev. **138B**, 979 (1965); K.F. Milfeld and R.E. Wyatt, Phys. Rev. A **27**, 72 (1983); N. Moiseyev and H.J. Korsch, *ibid.* **44**, 7797 (1991); B. Galdrikian, M. Sherwin, and B. Birnir, Phys. Rev. B **49**, 13 744 (1994).

[5] F. Großmann and P. Hänggi, Europhys. Lett. **18**, 571 (1992); J.M.G. Llorente and J. Plata, Phys. Rev. A **45**, R6958 (1992); Y. Dakhnovskii and R. Bavli, Phys. Rev. B **48**, 11 020 (1993).

[6] T. Dittrich, B. Oelschlägel, and P. Hänggi, Europhys. Lett. **22**, 5 (1993); Y. Dakhnovskii, Phys. Rev. B **49**, 4649 (1994).

[7] D. Farrelly and J.A. Milligan, Phys. Rev. E **47**, R2225 (1993); L. Sirko, S. Yoakum, A. Haffmans, and P.M. Koch, Phys. Rev. A **47**, R782 (1993).

[8] M. Holthaus, Z. Phys. B **89**, 251 (1992); Phys. Rev. Lett. **69**, 351 (1992); M. Holthaus and D. Hone, Phys. Rev. B **47**, 6499 (1993).

[9] M. Wagner, Phys. Rev. B **49**, 16 544 (1994).

[10] Antti-Pekka Jauho, Phys. Rev. B **41**, 12 327 (1990); W. Cai, T.F. Zheng, P. Hu, M. Lax, K. Shum, and R.R. Alfano, Phys. Rev. Lett. **65**, 104 (1990); Y. Fu and M. Willander, J. Appl. Phys. **72**, 3592 (1992); J. Iñarrea, G. Platero, and C. Tejedor, Semicond. Sci. Technol. **9**, 515 (1994).

[11] M. Büttiker and R. Landauer, Phys. Rev. Lett. **49**, 1739 (1982); IBM J. Res. Dev. **30**, 451 (1986).

[12] P.K. Tien and J.P. Gordon, Phys. Rev. **129**, 647 (1963).

[13] Q. Hu, Appl. Phys. Lett. **62**, 837 (1993); R.A. Wyss, C.C. Eugster, J.A. del Alamo, and Q. Hu, *ibid.* **63**, 1522 (1993); S. Feng and Q. Hu, Phys. Rev. B **48**, 5354 (1993).

[14] F. Hekking and Yu.V. Nazarov, Phys. Rev. B **44**, 9110 (1991); **44**, 11 506 (1991).

[15] J.D. White and M. Wagner, Phys. Rev. B **48**, 2799 (1993).

[16] C. Bruder and H. Schoeller, Phys. Rev. Lett. **72**, 1076 (1994).

[17] L.P. Kouwenhoven S. Jauhar, K. McCormick, D. Dixon, P.L. McEuen, Yu.V. Nazarov, N.C. van der Vaart, and C.T. Foxon, Phys. Rev. B **50**, 2019 (1994).

[18] M. Wagner and H. Mizuta, Phys. Rev. B **48**, 14 393 (1993).

[19] N.S. Wingreen, K.W. Jacobsen, and J.W. Wilkins, Phys. Rev. Lett. **61**, 1396 (1988); B.Y. Gelfand, S. Schmitt-Rink, and A.F.J. Levi, *ibid.* **62**, 1683 (1989); W. Cai, T.F. Zheng, P. Hu, B. Yudanin, and M. Lax, *ibid.* **63**, 418 (1989).

[20] Note that, averaged over time, the displacement current vanishes. It is only in the ac response where the displacement current matters. See, for instance, M. Büttiker, A. Prêtre, and H. Thomas, Phys. Rev. Lett. **70**, 4114 (1993); M. Büttiker and H. Thomas, in *Quantum-Effect Physics, Electronics and Applications*, edited by K. Ismail *et al.*, Institute of Physics Conference Series No. 127 (Hilger, Bristol, 1992), p. 19.

[21] This "sequential" picture also explains why in a *symmetric* double-barrier structure the transmission and reflection probabilities are the same in any sideband $n \neq 0$.

[22] Note that for the special case of ν being integer, Eq. (B6) reproduces the symmetry $T_{-\nu,n-\nu} = T_{-\nu,\nu-n}$ found in the resonant case.

[23] A. Larsson, S.I. Borenstain, B. Jonsson, I. Andersson, J. Westin, and T.G. Andersson, Appl. Phys. Lett. **58**, 1297 (1991).

[24] The situation is completely different when the driving

field can excite transitions between different resonances of the system; cf. F. Großmann and P. Hänggi, Chem. Phys. **170**, 295 (1993).

[25] As the tunneling is completely coherent, the transmission probability for an electron to tunnel from left to right is exactly the same as for the reverse direction, even in the presence of a driving field. Therefore, the photon-assisted tunneling depends equally well on the driving fields at the input and the output side of the diode. Rectification of the photon-assisted current occurs only for sequential tunneling.

[26] A perturbative treatment of the transfer matrices up to first order in the driving field was given in H.C. Liu, Phys. Rev. B **43**, 12 538 (1991); special cases of strongly driven double- and triple-barrier structures were considered in O. Olendskii, Phys. Lett. A **161**, 170 (1991); Zh. Tekh. Fiz. **62**, 92 (1992) [Sov. Phys. Tech. Phys. **37**, 46 (1992)].

[27] In the Floquet theory, this corresponds to the quasi-energy being restricted to the first "Brillouin zone" $\{-\hbar\omega/2, \hbar\omega/2\}$.

[28] *Pocketbook of Mathematical Functions*, edited by M. Abramowitz and I.A. Stegun (Verlag Harry Deutsch, Thun, 1984); R. Courant and D. Hilbert, *Methoden der Mathematischen Physik I* (Springer-Verlag, Berlin, 1968).

[29] Note that this is different from the convention used in Ref. [9], where the reference energy was always taken to be the energy of the quantum-well resonance.

[30] Of course, this ansatz reduces to the one given in Ref. [9] for integer ν.